J Mater Sci (2008) 43:3320–3326
DOI 10.1007/s10853-008-2503-7

Redox processes at grain boundaries in barium titanate-based polycrystalline ferroelectrics semiconductors

Antolii Belous · Oleg V'yunov · Maya Glinchuk · Valentin Laguta · Darko Makovez

Received: 3 September 2007 / Accepted: 25 January 2008 / Published online: 5 March 2008

Abstract Barium titanate, which is characterized by a positive temperature coefficient of resistance (PTCR), is widely used in practice. At the same time, it is unknown why only a small percentage of the introduced donor dopant takes part in the formation of PTCR effect, which phases appear at grain boundaries, how the introduced acceptor dopants affect the properties of grains. Elucidation of the above questions is of considerable scientific and practical interest. It has been shown that the phases $Ba_6Ti_{17}O_{40}$ and $Y_2Ti_2O_7$ precipitate on grains of barium titanate doped with donor dopant (yttrium). We identified paramagnetic impurities (iron, manganese, chromium) in starting reagents. These impurities can occupy titanium sites. Therefore, the part of the donor dopant that is spent on the charge exchange of acceptor dopants does not participate in the charge exchange of titanium $Ti^{4+} \rightarrow Ti^{3+}$, which is responsible for the appearance of PTCR effect in barium titanate. It has been found that an extra acceptor dopant (manganese) is distributed mainly at grain boundaries and in the grain outer layer. It has been shown that manganese ions introduced additionally (as acceptor dopants) increase the potential barrier at grain boundaries and form a high-resistance outer layer in PTCR ceramics. The resistance of grains, outer layers, and grain boundaries as a function of the manganese content has been investigated.

A. Belous · O. V'yunov (✉)
V.I. Vernadskii Institute of General and Inorganic Chemistry, Kyiv, Ukraine
e-mail: vyunov@ionc.kar.net

M. Glinchuk · V. Laguta
Frantsevich Institute for Problems of Materials Sciences, Kyiv, Ukraine

D. Makovez
Jožef Stefan Institute, Ljubljana, Slovenia

Introduction

Barium metatitanate, which is characterized by a positive temperature coefficient of resistance, is widely used in engineering. One of the conditions for the appearance of the above effect is potential barrier formation at grain boundaries. Therefore, in the synthesis of materials in which PTCR effect manifests itself, conditions are purposively created at which high-resistance boundaries and semiconductive ceramic grains are formed. This is achieved by partial substitution of barium by three-valent ions (for example, Y, La, Nd, etc.) [1, 2] or titanium by ions of the fifth or sixth group (for example, Nb, Ta, Mo, etc.) [3, 4]. At the same time many questions remain not elucidated. For instance, it is unknown: (1) on what processes that occur during the formation of PTCR materials and in what proportions the introduced rare-earth ions (e.g. yttrium ions) are spent; (2) what extra phases are formed at grain boundaries; (3) how the acceptor dopants introduced additionally affect the properties of grains, grain boundary, and the outer layer (the intermediate region between grain and grain boundary). It is to the elucidation of these questions that this article is devoted.

An important process in the formation of PTCR properties during sintering in air is the oxidation of grain boundaries on cooling. It is difficult to investigate these oxidation processes using diffraction methods because the doping level does not exceed one percent, and only outer layers of grains are usually oxidized. To investigate the processes occurring at grain boundaries, the oxidation

processes in the reduced form of fine-grained powders can be investigated supposing that the same processes occur at grain boundaries. In fine-grained powders, the oxidized area increases substantially, resulting in an increase in the percentage of the phases, which are formed on oxidation and, therefore, it is possible to use diffraction methods for the investigation of phase composition. It is known that, in comparison to the synthesis in air, the degree of substitution of rare-earth elements for barium ions is higher when barium titanate is synthesized in a reducing atmosphere. Therefore, by investigating the reduced form of barium titanate after oxidation it is possible to obtain information about the phases, which are formed at grain boundaries. This approach was used by the authors of [9] for investigations of microstructural changes during oxidation of the reduced form of lanthanum-doped barium titanate. Although yttrium-doped barium titanate has good electrophysical characteristics, the redox processes during its synthesis are not described in the literature.

Experimental

Extra-pure $BaCO_3$ (purity 99.999%),[1] TiO_2 (rutile, purity 99.99%),[2] and Y_2O_3 (purity 99.99%)[3] were used as initial reagents. The powders were mixed in the 1:1.02:x ratio ($x = 0.004-0.025$) and ball-milled in an agate mortar. The mixtures were granulated with the addition of 10% polyvinyl alcohol, pressed into pellets (10 mm in diameter and 2 mm in thickness) by uniaxial pressing at 150 MPa, and sintered under reduction conditions ($P_{O_2} = 10^{-4}$ Pa) at 1,400 °C for 4 h. The heating and cooling rates for all samples were 300 °C h^{-1}. Under these conditions, yttrium is incorporated into barium titanate lattice in amounts sufficient for X-ray analysis (yttrium solubility limit under these conditions reaches ca. 4 mol% Y_{Ba} [5], while in the case of sintering in air it does not exceed 1.5 mol% Y_{Ba} [6]). The samples with an yttrium content of 1 mol% (less than solubility limit in the case of synthesis in air) and 2.5 mol% (more than solubility limit in the case of synthesis in air, but less than solubility limit at $P_{O_2} = 10^{-4}$ Pa) were chosen for investigation. The ratios of cation contents measured using wave-dispersion spectroscopy (WDS) in grains of solid solutions were in good agreement with the nominal compositions of the samples. As-fired ceramic pellets and powder after grinding and milling of ceramic pellets and sifting through a nylon mesh with 40 × 40 μm grid were used for oxidation. Samples were oxidized at 1,150 °C for 20 h. The powders were used for X-ray investigations, and the tablets were used for electron microscopy.

The phases precipitated during the oxidation process were characterized by X-ray powder diffractometry (XRPD) using DRON-4-07 (Cu $K\alpha$ radiation; 40 kV, 20 mA) and transmission electron microscopy (TEM) using JEM 2000 FX, JEOL, Tokyo, Japan (LaB_6 cathode; accelerating voltage, 200 kV). Bright-field (BF) and dark-field (DF) imaging in combination with selected area electron diffraction (SAED), microdiffraction (MD), and electron-dispersive X-ray spectroscopy (EDXS) were used.

Impedance data were obtained using a 1260 Impedance/Gain-phase Analyzer (Solartron Analytical) in the range 100 Hz to 1 MHz and a VM-560 Q-meter in the range 50 kHz to 35 MHz. The components of the equivalent circuit were identified using the Frequency Response Analyzer 4.7 program.

Electron-spin resonance (ESR) spectra were recorded using a spectrometer operating at a microwave frequency of 9.2–9.4 GHz.

Results and discussion

Undoped barium titanate is known to have a high resistivity (10^{10}–10^{12} Ω cm) [7]. On partial substitution of rare-earth ions (e.g. yttrium ions) for barium ions, the resistivity decreases by several orders of magnitude, and the ceramic becomes conducting.

The highest conductivity of Y-doped barium titanate at room temperature is 10 Ω^{-1} m^{-1}, which is in good agreement with literature data [7]. An yttrium concentration of the order of 5 10^{25} m^{-3} (2,000–4,000 ppm) is necessary for this. Measurements of thermal emf and Hall effect [8] showed that the electron mobility (μ) in $BaTiO_3$ is 5 × 10^{-5} m^2 V^{-2} s^{-1}. The conductivity σ is given by $\sigma = e\ n\ \mu$, where e is electron charge of 1.6 × 10^{-19} C, n is the electron concentration, and μ is the electron mobility. Using the above equation, the conduction electron concentration can be determined. This allows the estimation of the concentration of the introduced yttrium, which gives rise to conduction. Calculations show the electron concentration to be (1–2) × 10^{24} m^{-3}, which is only 2–5% of the donor (yttrium) concentration.

It is clear that some amount of the yttrium ions can be spent on charge exchange of paramagnetic impurities, which are usually present in starting reagents. We used ESR measurements to find out the sort of the paramagnetic impurities introduced into synthesized $BaTiO_3$ ceramics. The measurements performed at room temperature on both

[1] Donetsk plant for chemical reagents, Donetsk, Ukraine; Manufacturer's analysis: Fe < 3 ppm, Mn < 3 ppm, Cu < 1 ppm.

[2] "Krasnyi Khimik'', St. Petersburg, Russia; Manufacturer's analysis: Fe < 3 ppm, Al < 2 ppm, Ca < 4 ppm.

[3] "Krasnyi Khimik'', St. Petersburg, Russia. Manufacturer's analysis: rare-earth oxides < 1 ppm, Fe_2O_3 < 3 ppm; CaO < 5 ppm; CuO < 1 ppm; PbO < 2 ppm.

pure and weakly doped barium titanate revealed well-known spectrum of Fe^{3+} [13] and a weak signal with a g-factor of 1.971–1.974 (Fig. 1). It should be noted that in the literature there are several interpretations of this ESR signal: intrinsic Ti^{3+}—related defect [10–11], charged barium vacancy defect [12]. Our last investigation [13] on both single crystal and ceramics of Cr-doped $BaTiO_3$ unambiguously proved that the ESR spectrum at $g = 1.971–1.974$ belongs to Cr^{3+} ions.

With increasing concentration of Y to 0.2–0.3% the intensity of the Fe^{3+} spectrum essentially decreases, while the intensity of the Cr^{3+} spectrum increases, reaching saturation at 0.1–0.2% Y. This can be explained by changing the valence state of iron and chromium due to the processes $Fe^{3+} + e \rightarrow Fe^{2+}$ and $Cr^{4+} + e \rightarrow Cr^{3+}$ because Y^{3+} leads to excess of positive charge in the lattice. Besides, when the Y content was increased, resonance lines of Mn^{2+} appeared as well. This indicates that yttrium ions participate in the charge exchange of manganese from Mn^{4+} and/or Mn^{3+} to Mn^{2+}.

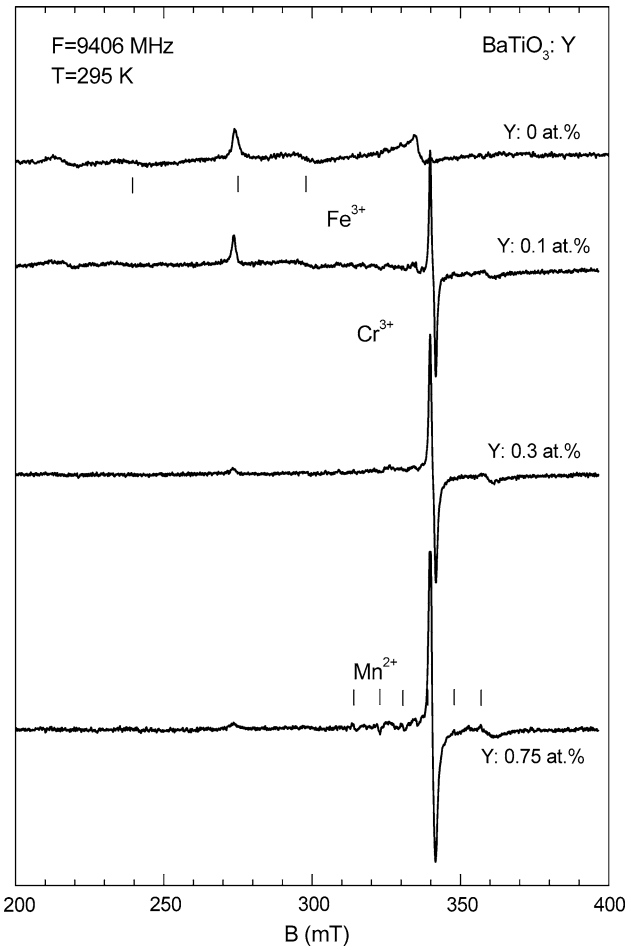

Fig. 1 ESR spectra of $Ba_{1-x}Y_x^{\bullet}TiO_3$ at room temperature

Thus, ESR measurements show that PTCR materials contain paramagnetic impurities of chromium, iron, and manganese. Their estimated concentrations are about 15, 200, and 100 ppm, respectively. In sum, it accounts only for 5–10% of the yttrium which is spent on the charge exchange of impurities.

To elucidate the processes on which the remaining amount of introduced yttrium is spent, we studied the phases that appear at grain boundaries in PTCR materials. It is known that semiconducting barium titanate doped with rare-earth ions as donor ions, e.g. yttrium ions, may be represented by the chemical formula $Ba_{1-x}Y_x^{\bullet}Ti_{1-x}^{4+}Ti_x^{3+}O_3$ (where $Ti^{3+} = Ti^{4+} + e^-$) [7]. This phase has a high conductivity, which is typical of semiconducting materials. During cooling after sintering, the ceramic is oxidized, and the dielectric oxidized form of barium titanate is formed, where cation vacancies arise for the compensation of the excess charge of donor dopant [9]. In Ref. [10] on the basis of atomistic simulation study of doping processes it was shown that the formation energy of $Y_{Ba}^{\bullet} + V_{Ti}^{''''}$ defect (4.35 eV) is lower than that of $Y_{Ba}^{\bullet} + V_{Ba}^{''}$ defect (7.23 eV). Therefore the oxidized form of yttrium-doped barium titanate may be represented as $Ba_{1-x}Y_x^{\bullet}Ti_{1-x/4}^{4+}(V_{Ti}^{''''})_{x/4}O_3$. This phase crystallizes as perovskite structure and appears at grain boundaries in PTCR materials. To investigate other phases, which may appear at grain boundaries during the formation of PTCR materials, we made use of diffraction and electron microscope investigations.

Figure 2 shows diffractograms of a sample of the reduced form of yttrium-doped barium titanate with the nominal formulas $Ba_{0.99}Y_{0.01}Ti_{0.99}^{4+}Ti_{0.01}^{3+}O_3$ and $Ba_{0.975}Y_{0.025}Ti_{0.975}^{4+}Ti_{0.025}^{3+}O_3$ before and after oxidation for 20 h at 1,150 °C in air. The diffractograms show that the samples of perovskite phase before and after oxidation are tetragonal (space group P4 mm [11]).

In the case of oxidation of ceramic samples for 20 h at 1,150 °C, only the areas near the surfaces of the pellets were light, while the inner areas of the pellets remained dark. Oxidation leads to the transition $Ti^{3+} \rightarrow Ti^{4+}$ and is accompanied by the lightening of the material. XRPD showed that the material inside the pellet was a single-phase one, whereas the material near the surface of the pellet was multiphase one (see Fig. 2, patterns 1′, 2′). In addition to the perovskite phase, the cubic compound $Y_2Ti_2O_7$ with pyrochlore structure (space group $Fd\bar{3}m$ (227) [12]) and monoclinic compound $Ba_6Ti_{17}O_{40}$ (space group C2/c (15) [13]) precipitated.

Figures 3–5 show micrographs of phases which precipitate on grains of ceramic of the nominal composition $Ba_{0.975}Y_{0.025}Ti_{0.975}{}^{4+}Ti_{0.025}{}^{3+}O_3$ after oxidation. Investigations of the microstructure of the ceramic show that in the sample with low yttrium concentration ($Ba_{0.99}Y_{0.01}$

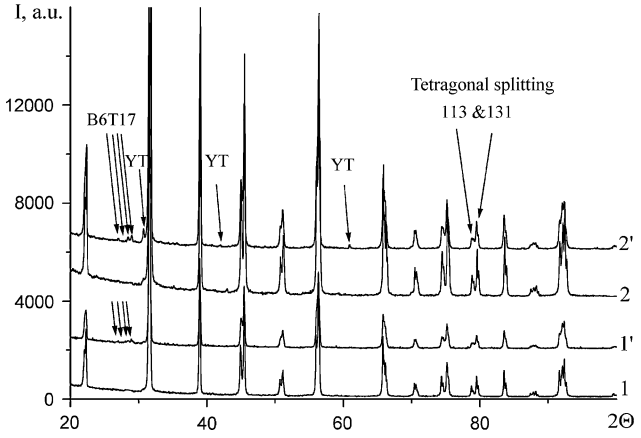

Fig. 2 Diffractograms of yttrium-doped barium titanate with the nominal compositions $Ba_{0.99}Y_{0.01}Ti^{4+}_{0.99}Ti^{3+}_{0.01}O_3$ (1, 1′) and $Ba_{0.975}Y_{0.025}Ti^{4+}_{0.975}Ti^{3+}_{0.025}O_3$ (2, 2′) after sintering in reducing atmosphere, $P_{O_2} = 10^{-4}$ Pa (1, 2) and after oxidation in air for 20 h at 1,150 °C (1′, 2′): BT = $BaTiO_3$, $B_6T_{17} = Ba_6Ti_{17}O_{40}$, YT = $Y_2Ti_2O_7$

$Ti^{4+}_{0.99}Ti^{3+}_{0.01}O_3$), as well as in the sample with high yttrium concentration $\left(Ba_{0.975}Y_{0.025}Ti^{4+}_{0.975}Ti^{3+}_{0.025}O_3\right)$ the $Ba_6Ti_{17}O_{40}$ phase precipitates after oxidation, which agrees with the XRPD results. The phase $Ba_6Ti_{17}O_{40}$ was located preferentially inside the matrix grains. It was found in two different forms. Figure 3 shows a TEM image of small bulk precipitates in an oxidized sample of the nominal composition $Ba_{0.975}Y_{0.025}Ti^{4+}_{0.975}Ti^{3+}_{0.025}O_3$. The precipitates are concentrated in a cluster, nearly rectangular in shape, which lies parallel to the {111} planes of the perovskite structure.

Investigations showed that the compound $Ba_6Ti_{17}O_{40}$ also precipitated in the form of thin platelike particles, lying in the perovskite close-packed {111} planes.

XRPD and electron microscopy showed that the second phase, which precipitated on the oxidation of a sample with a high yttrium concentration, $Ba_{0.975}Y_{0.025}Ti^{4+}_{0.975}Ti^{3+}_{0.025}O_3$, was the $Y_2Ti_2O_7$ phase. The precipitates of this phase were found in two different shapes. Figure 4 shows a small precipitate (~0.2 μm in size) in an oxidized sample with the nominal composition$Ba_{0.975}Y_{0.025}Ti^{4+}_{0.975}Ti^{3+}_{0.025}O_3$. This precipitate has a cuboid shape. TEM analysis suggested that there is a certain orientational relationship between the precipitate and the perovskite matrix since the outer surfaces of cubic precipitate lie parallel to the {100} plane of perovskite grain.

In addition to rectangular bulk precipitates, the $Y_2Ti_2O_7$ phase was also found in globular shape. Figure 5 shows a spherical precipitate of ~1 μm size, and SAED shows that it is oriented in the ⟨211⟩ direction.

These investigations show that in PTCR ceramics with low yttrium concentration $Ba_{0.99}Y_{0.01}Ti^{4+}_{0.01}Ti^{3+}_{0.01}O_3$, the phases $Ba_{1-x}Y_xTi^4_{1-x/4}(V_{Ti})_{x/4}$ and $Ba_6Ti_{17}O_{40}$ appear at grain boundaries. When the yttrium concentration is increased, an extra phase $Y_2Ti_2O_7$ is formed at grain boundaries. These phases are characterized by dielectric properties, and yttrium is spent on their formation.

It is known that the introduction of acceptor dopants (for example, manganese) in synthesized materials improves the above characteristic of PTCR barium titanate [14, 15]. The effect of manganese additive on the properties of PTCR materials based on barium titanate was investigated in a number of works [14, 16–20]. It has been shown that manganese is located at grain boundaries and acts as acceptor dopant, increasing the order of magnitude of resistivity change in the area of PTCR effect [14]. Introduction of manganese in PTCR ceramics based on barium titanate changes the energy of acceptor states [16, 17]. Manganese forms a number of associates with oxygen vacancies, which act at grain boundaries as acceptorlike centers of electron capture [18]. In the case of partial substitution of titanium ions by manganese ions in barium titanate, the samples become bimodal at manganse contents of over 1 mol%, and in the range of 0.5–1.7 mol% the coexistence of tetragonal and hexagonal perovskite phases is observed [19]. However, information about the

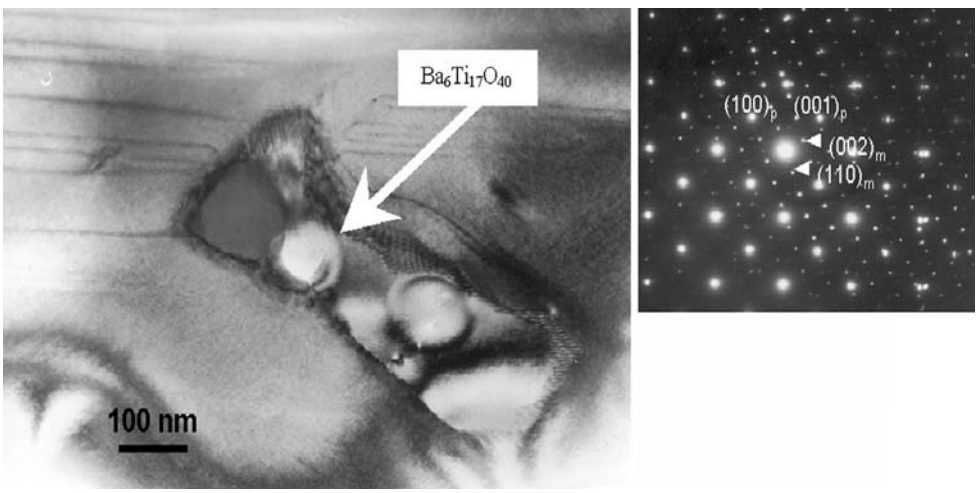

Fig. 3 (**a**) Micrograph of $Ba_6Ti_{17}O_{40}$ phase in the matrix grain of a sample of the nominal composition $Ba_{0.975}Y_{0.025}Ti^{4+}_{0.975}Ti^{3+}_{0.025}O_3$, which precipitates after oxidation in air for 20 h at 1,150 °C. (**b**) Electron diffraction pattern taken in the region of the grain with precipitate

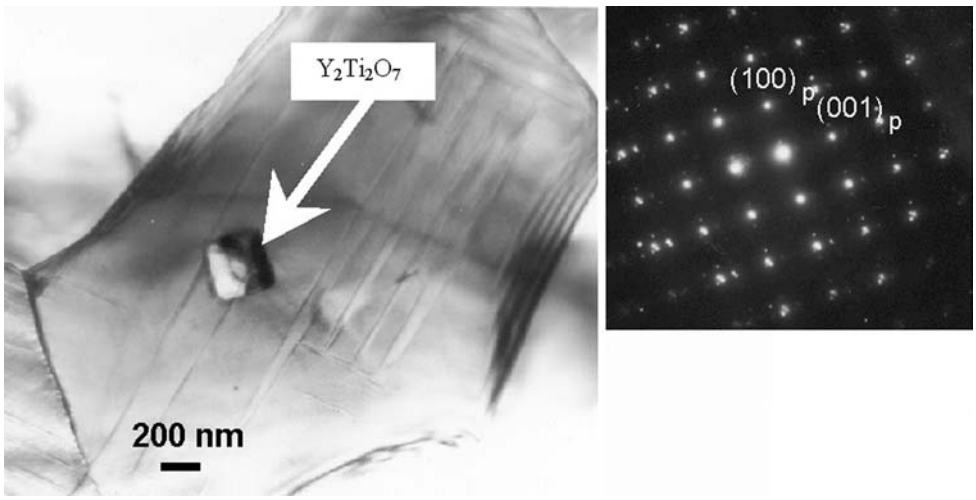

Fig. 4 (**a**) Micrograph of rectangular $Y_2Ti_2O_7$ phase in the matrix grain of a sample of the nominal composition $Ba_{0.975}Y_{0.025}Ti^{4+}_{0.975}Ti^{3+}_{0.025}O_3$, which precipitates after oxidation in air for 20 h at 1,150 °C. (**b**) Electron diffraction pattern taken in the region of the grain with precipitate, marked by an arrow in (**a**)

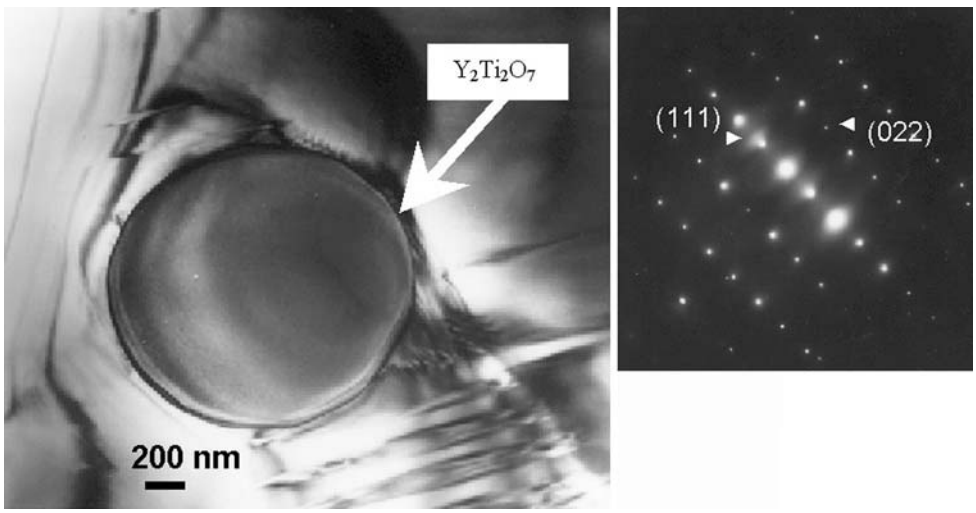

Fig. 5 (**a**) Micrograph of spherical $Y_2Ti_2O_7$ phase in the matrix grain of a sample of the nominal composition $Ba_{0.975}Y_{0.025}Ti^{4+}_{0.975}Ti^{3+}_{0.025}O_3$, which precipitates after oxidation in air for 20 h at 1,150 °C. (**b**) Electron diffraction pattern taken at the precipitate

distribution of manganese dopant and its effect on the properties of grain, boundary, and the outer layer in polycrystalline material is scantily presented in the literature.

Electron micrographs of $(Ba_{0.996}Y_{0.004})TiO_3$ ceramic without and with the manganese dopant sintered in air for 2 h are shown in Fig. 6. The average grain size of barium-titanate-based ceramic is ca. 35 μm.

The temperature dependence of resistivity of PTCR ceramics may be divided schematically into 3 ranges (Fig. 7). Range I extends from room temperature to the phase transition temperature and is characterized by relatively low resistivity, which decreases with temperature (the temperature dependence demonstrates semiconductor behavior). Range II is situated over the phase transition temperature, where a rapid growth of resistivity is observed (PTCR effect). Range III exists at higher temperatures and is characterized by high resistivity, which decreases with temperature. When PTCR ceramics based on barium titanate are doped with manganese, the order of magnitude of resistivity change in the PTCR area increases (see Fig. 7, range II).

The results of frequency investigation of the PTCR ceramics based on barium titanate can be analyzed from four types of dependences: complex impedance (Z*), complex admittance (Y*), complex permittivity (ε*), and complex electric modulus (M*) [21–23].

The resistances of grain, the outer layer, and grain boundary of the PTCR ceramic $(Ba_{0.996}Y_{0.004})TiO_3$ without manganese dopant were calculated from the experimental data (Fig. 8a). The temperature dependence of the outer layer resistance of $(Ba_{0.996}Y_{0.004})TiO_3$ ceramic is of the character similar to that of grain and demonstrates no anomalies (Fig. 8a, curves 2, 3), whereas that of grain boundary displays anomalies. Formation of outer layer in the PTCR ceramics without manganese dopant occurs due to the diffusion of oxygen into grains on cooling. In this case the trivalent titanium ions partially change to tetravalent ones in the outer layer, resulting in an increase in the electrical resistivity of this layer [24]. Hence, the PTCR effect in $(Ba_{0.996}Y_{0.004})TiO_3$ ceramic without manganese dopant occurs due to a

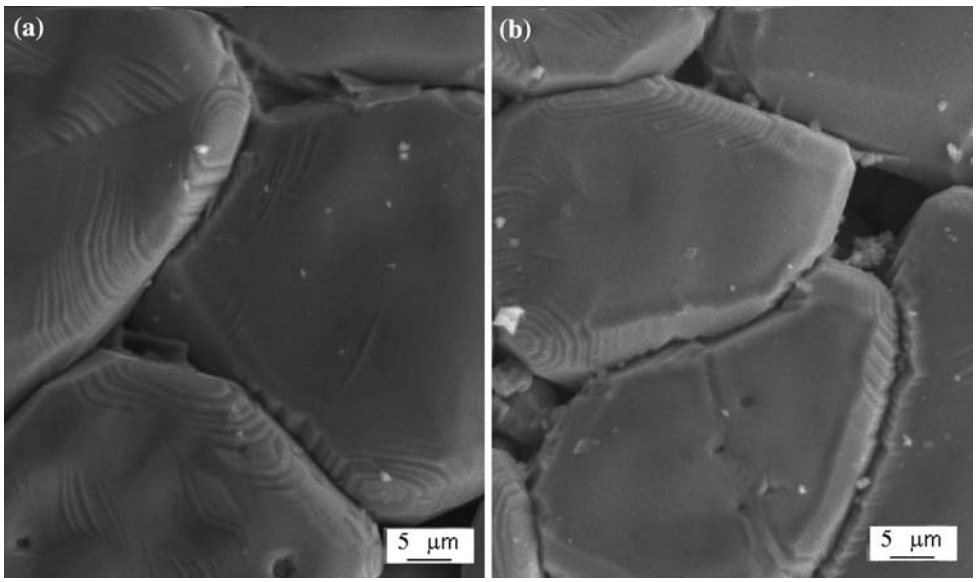

Fig. 6 Microstructure of the PTCR ceramics $(Ba_{0.996}Y_{0.004})TiO_3$ (**a**); $(Ba_{0.996}Y_{0.004})TiO_3$ + 0.006 mol% Mn (**b**). Scale bar = 10 μm

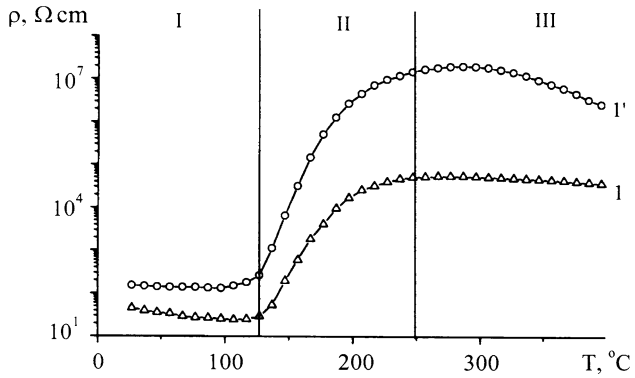

Fig. 7 Resistivity (ρ) of the PTCR ceramics (Ba,Y)TiO_3 (1); (Ba,Y)TiO_3 + 0.006 mol% Mn (1′) versus temperature. I, II and III are the ranges with different character of dependences ρ(T)

change in electrophysical properties of grain boundaries (Fig. 8a, curve 1).

The resistance of grain, the outer layer, and grain boundary of the PTCR ceramics $(Ba_{0.996}Y_{0.004})TiO_3$ and $(Ba_{0.996}Y_{0.004})TiO_3$ + 0.006 mol% Mn is shown in Fig. 8 b. The character of the variation of the outer layer resistance of the ceramic $(Ba_{0.996}Y_{0.004})TiO_3$ + 0.006 mol% Mn with temperature is similar to that of the variation of grain boundary resistance in contrast to the ceramics without manganese dopant (Fig. 8a, curves 2, 3). This is probably due to the fact that manganese partially diffuses into the grain outer layer [25].

Conclusions

Thus, in Y-containing $BaTiO_3$−based PTCR ceramics, the introduced yttrium is spent on various processes. For instance, 2–5% of the introduced yttrium is involved in the charge exchange of titanium ($Ti^{4+} + e^- \leftrightarrow Ti^{3+}$), which leads to an increase in conductivity. 5–10% of yttrium participates in the charge exchange of paramagnetic impurities (chromium, iron, manganese ions) which are present in the starting reagents. The remaining yttrium is present in the phases at grain boundaries ($Ba_{1-x}Y_x^{\bullet}$ $Ti_{1-x}^{4+}Ti_x^{3+}O_3$, $Ba_6Ti_{17}O_{40}$ and $Y_2Ti_2O_7$), which are characterized by dielectric properties.

PTCR ceramic of $(Ba_{0.996}Y_{0.004})TiO_3$ system has a coarse-grained microstructure. When adding manganese dopant, manganese ions diffuse into the grain, essentially

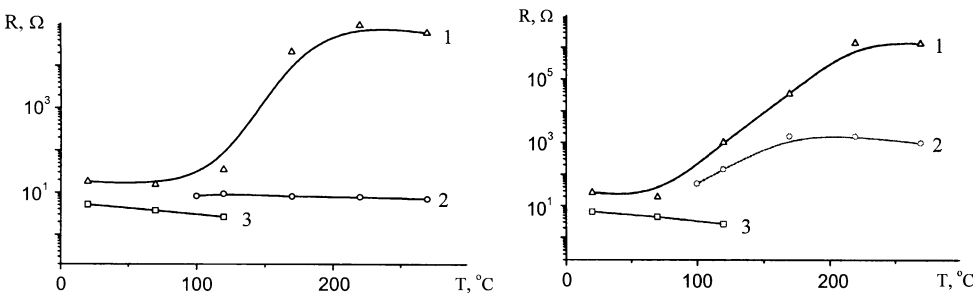

Fig. 8 Resistance of grain boundary (1), outer layer (2) and grain (3) of PTCR ceramics (Ba,Y)TiO_3 (**a**) and (Ba,Y)TiO_3 + 0.006 mol% Mn (**b**) versus temperature

changing the properties of grain outer layers. At the same time, the electrophysical properties of grain core and grain boundaries change slightly.

The utilized methodology of the investigation of redox processes and grain boundary phases allows one to study the systems with low dopant concentrations as well as to intentionally control the PTCR properties of barium-titanate-based materials, when they may contribute to extending the range of their application.

References

1. Saburi O (1959) J Phys Soc Jpn 14:1159
2. Tennery VJ, Cook RL (1961) J Amer Ceram Soc 44(4):187
3. Rotenberg BA, Yu L, Danilyuk (1967) Izv AN SSSR Ser Fiz 31(11):1824
4. Belous AG, V'yunov OI, Khomenko BS (1998) Inorg Mater 34(6):725
5. Kostikova GP, Kostikov YP (1997) Chemical processes during doping of oxides, St. Petersburg, 156 p
6. Zhi J, Chen A, Zhi Y, Vilarihno PM, Baptista JL (1999) J Am Ceram Soc 82(5):1345
7. Okazaki O (1977) Semiconducting barium titanate, Tokyo, Gakkensya
8. Heywang V (ed) (1987) Amorphous and polycrystalline semiconductors (trans: Heywang V, Birkholtz U, Aintziger R et al (Germ)) Moscow, Mir, 160 p
9. Makovec D, Drofenik M (2000) J Am Ceram Soc 83(10):2593
10. Buskaglia MT, Buskaglia V, Viviani M, Nanni P (1998) Doping of $BaTiO_3$ with rare-earth oxide, 9th international conference on modern materials & technologies. Florence, Italy
11. Evans HT (1961) Acta Cryst 14:1019
12. Kato M, Kubo T (1967) J Chem Soc Jpn 70(6):840
13. Negas T, Roth RS, Parker HS, Minor D (1981) J Solid Stale Chem 9:287
14. Al-Allak HM, Brinkman AW, Russel GJ, Woods J (1988) J Appl Phys 63(9):4530
15. Lee JH, Kim SH, Cho SH (1995) J Amer Ceram Soc 78(10):2845
16. Huybrechts B, Ishizaki K, Takata M (1992) J Am Ceram Soc 75:722
17. Huybrechts B, Takata M, Ishizaki K (1994) Ceram Transact Am Ceram Soc 44:151
18. Miki T, Fudjimoto A, Jida S (1998) J Appl Phys 83(3):1592
19. Langhammer HT, Muller T, Felgner K-H, Abich H-P (2000) J Am Ceram Soc 83(3):605
20. Langhammer HT, Muller T, Felgner K-H, Abich H-P (2000) Mater Lett 42:21
21. Sinclair DC, Morrison FD, West AR (2000) International Ceramics 2:33
22. Morrison FD, Sinclair DC, West AR (2001) J Am Ceram Soc 84(2):474
23. Morrison FD, Sinclair DC, West AR (2001) J Am Ceram Soc 4(3):531
24. Morrison FD, Coats AM, Sinclair DC, West AR (2001) J Electroceram 6(3):219
25. Altbersen K, Hennings D, Steigelmann O (1998) J Electroceram 2–3:193